Eur. Phys. J. C (2015) 75:161
DOI 10.1140/epjc/s10052-015-3381-1

THE EUROPEAN PHYSICAL JOURNAL C

CrossMark

Regular Article - Theoretical Physics

Mass reach scaling for future hadron colliders

Thomas G. Rizzo[a]

SLAC National Accelerator Laboratory, Menlo Park, CA 94025, USA

Received: 29 January 2015 / Accepted: 31 March 2015 / Published online: 24 April 2015

Abstract The primary goal of any future hadron collider is to discover new physics (NP) associated with a high mass scale, M, beyond the range of the LHC. In order to maintain the same *relative* mass reach for rate-limited NP, $M/\sqrt{s}$, as $\sqrt{s}$ increases, Richter recently reminded us that the required integrated luminosity obtainable at future hadron colliders (FHC) must grow rapidly, $\sim s$, in the limit of naive scaling. This would imply, e.g., a ∼50-fold increase in the required integrated luminosity when going from the 14 TeV LHC to a FHC with $\sqrt{s} = 100$ TeV, an increase that would prove quite challenging on many different fronts. In this paper we point out, due to the scaling violations associated with the evolution of the parton density functions (PDFs) and the running of the strong coupling, α_s, that the actual luminosity necessary in order to maintain any fixed value of the relative mass reach is somewhat greater than this scaling result indicates. However, the actual values of the required luminosity scaling are found to be dependent upon the detailed nature of the NP being considered. Here we elucidate this point explicitly by employing several specific benchmark examples of possible NP scenarios and briefly discuss the (relatively weak) search impact in each case if these luminosity goals are not met.

1 Introduction and background

There is rising interest in the physics potential of a future higher energy hadron collider which might begin running sometime after the high luminosity LHC program is completed. Such a machine, here generically termed the FHC, has been discussed in various manifestations at a growing number of workshops.[1] but generally is expected to operate in the $\sqrt{s} \sim 100$ TeV energy range. The goal of such a machine will be to explore the unknown, i.e., to search for new physics (NP), both beyond the standard model (SM) and beyond the reach of the LHC, that might be kinematically accessible at these higher collision energies. As such, its NP search capabilities should be as strong as possible, and in particular be at least as powerful as those we expect to be available at the 14 TeV LHC. This NP may take several forms: it may be relatively light but very weakly coupled to the SM so that the increased cross sections at a higher energy collider will allow access. More commonly, we imagine this NP to manifest as some new, very heavy state(s), simply too massive to be produced at the 14 TeV LHC; this is the case we will consider below.

Searches for NP can be quite complex, generally involving sophisticated experimental analyses in order to extract a significant signal above some SM background. This makes quantifying the power of a future collider difficult without a detailed study of a wide range of potential NP physics scenarios. Depending on what kind of NP one is interested in various possibilities come to mind. Here, as said above, we are essentially only interested in NP which is quite heavy. Perhaps in this case a crude but simple measure of this potential discovery power is obtainable by employing the value of the *relative* mass reach in the case of a rate-limited signal for NP[2] associated with a heavy mass scale M, i.e., the value of the mass reach scaled to the collision energy, $M/\sqrt{s}$. For example, this would mean that if a new 3.5 TeV state is dis-

[a] e-mail: rizzo@slac.stanford.edu

[1] See, for example, the several long-term studies and associated conferences and workshops that have been recently started in both Europe and China: CERN SFCC Study: https://espace2013.cern.ch/fcc/Pages/default.aspx, Chinese Study on CEPC-SppC: http://cfhep.ihep.ac.cn/. There have also been workshops in the US in 2014 on such higher energy hadron colliders, e.g.,: https://indico.fnal.gov/conferenceDisplay.py?confId=7633 and https://indico.fnal.gov/conferenceOtherViews.py?view=standard&confId=7864.

[2] In the case of a background-limited signal the required luminosity would need to grow significantly faster with the collision energy $\sim s^2$.

coverable with some fixed number of signal events at the 14 TeV LHC then the corresponding 25 TeV state should be discoverable at the 100 TeV FHC with the same number of events. We can achieve this by requiring that as the $\sqrt{s}$ increases the number of NP events remains at (or above) the given fixed reference value. To accomplish this it is clear that the integrated luminosity, L, of the collider must grow with increasing $\sqrt{s}$. Richter has recently emphasized this issue [1] and reminded us that in the scaling limit for the NP cross section, σ, L must grow as $\sim s$, the square of the collider center of mass energy. In such a limit, the relevant ratio of appropriately *energy-scaled* cross sections is given by

$$R = \frac{\sigma(M/\sqrt{s},\ s)}{\sigma(M/\sqrt{s},\ s = s_0)}\ \frac{s}{s_0} \tag{1}$$

which is defined for a *fixed* value of the ratio $M/\sqrt{s}$ and by a reference collision energy, $\sqrt{s_0}$.[3] Note that the value of R is then simply unity in the scaling limit, by construction, reflecting the required luminosity growth as discussed above.

Of course we know that exact scaling is broken in the real world arising from a number of sources, e.g., due to the evolution of the parton density functions (PDFs) and the running of the strong coupling, α_s. (We note that the running of the other SM couplings, such as $\alpha_{\rm weak}$, while also producing a small scaling violation, will not play too large of a numerical role here.) This implies that the ratio R depends on $\sqrt{s}$ even for fixed values of $M/\sqrt{s}$ for any realistic NP signal process. In fact, as we will discuss below, we will find that it is always true that both these sources of scaling violation will force $R < 1$ for any $\sqrt{s} > 14$ TeV. This subsequently implies that even greater increases in integrated luminosities will be required to maintain the same relative mass reach than what is suggested by the naive scaling argument made above. Specifically, we will show that, roughly speaking, over the $\sqrt{s}$ range of interest, the ratio R scales as $\sim(\sqrt{s})^{-p}$ with $p > 0$, although this crude approximation breaks down over larger ranges of collision energy. Thus instead of the naive scaling of the needed luminosity $L_{NS} \sim (\sqrt{s})^2$, the actual luminosity scaling required to maintain the same relative mass reach is larger and is given approximately as $L \sim (\sqrt{s})^{2+p}$. As we will see below, for some processes p can be as large as $\sim$0.6 which implies a significant increase in the value of the desired luminosity. Thus the value of $1/R$ tells us the *additional* multiplicative factor that one needs to apply, beyond that obtained from simple scaling, in order to maintain the same relative mass reach as we increase $\sqrt{s}$. Of course, in actuality we will find that p is only approximately constant in each case and it, itself, also increases slowly with $\sqrt{s}$. However, we will see that the larger the roles of α_s and the gluon PDF are in the NP production cross section the greater the value of p and the larger the requited integrated luminosity will be to maintain the scaled mass reach will be.

Given these numerical results it will be the subject of further future studies to decide if the benefits of achieving this desired luminosity goal are worth the associated costs. Note that in the discussion below we will not address in any great detail the issue of the consequences to the various NP search reaches in the event that the corresponding integrated luminosity goals are not met at a future collider; we will, however, providing several examples. From these few cases it would seem that the impact of falling short of these goals, while limiting, still results in an enormous gain in search reach. However, more detailed work needs to be performed to fully access this very important problem. These are not new issues; discussions such as these took place over 30 years ago at the beginning of the SSC era [2].

2 Effects of PDF scaling violations and α_s running

To begin this discussion it is useful to examine how the ratio R is influenced purely by the evolution of the PDFs themselves. In order to be definitive, we will employ the recently available default 5-flavor NNLO MMHT2014 set of PDFs [3] as well as their corresponding default NNNLO running value of α_s assuming that $\alpha_s(M_Z) = 0.118$ in the numerical analysis that appears below. It should be noted, however, that the results we obtain can easily be shown to be quite insensitive to these particular choices. In order to access these effects, we consider the standard integrated products of the parton densities, i.e., the parton luminosities:

$$\mathcal{L}_{ij} = \int_\tau^1 {\rm d}x \left(f_i(x, M^2) f_j(\tau/x, M^2) + i \leftrightarrow j \right)/x \tag{2}$$

where f_i is the relevant PDF, $\tau = M^2/s$ and with M being identified with the partonic invariant mass at which the PDFs are evaluated. Depending upon the nature of NP, different combinations of the PDFs are usually involved. Here, to provide some specific examples we consider four sample cases: (i) we perform a sum over i, j pairs corresponding to the product of $Q = 2/3$ quarks and anti-quarks, denoted as $U\bar{U} = u\bar{u} + c\bar{c}$, (ii) we instead sum over the corresponding products of $Q = -1/3$ quarks and anti-quarks, denoted as $D\bar{D} = d\bar{d} + s\bar{s} + b\bar{b}$, (iii) the product of the gluon density with a sum over all the quark and anti-quark densities, denoted as $qG = g(u + \bar{u} + d + \bar{d} + \cdots)$, and lastly (iv) the product of two gluon densities, noted as gg. For each of these cases we fix the values of $M/\sqrt{s}$ and then determine the corresponding ratios $\mathcal{L}(\sqrt{s})/\mathcal{L}(\sqrt{s} = 14\ {\rm TeV})$ as $\sqrt{s}$ is increased. These ratios are, of course, all unity in the scaling limit. The results of these calculations are shown in Fig. 1 to which we now turn.

[3] Here, since we will be making comparison with the LHC it will be convenient to take $\sqrt{s_0} = 14$ TeV.

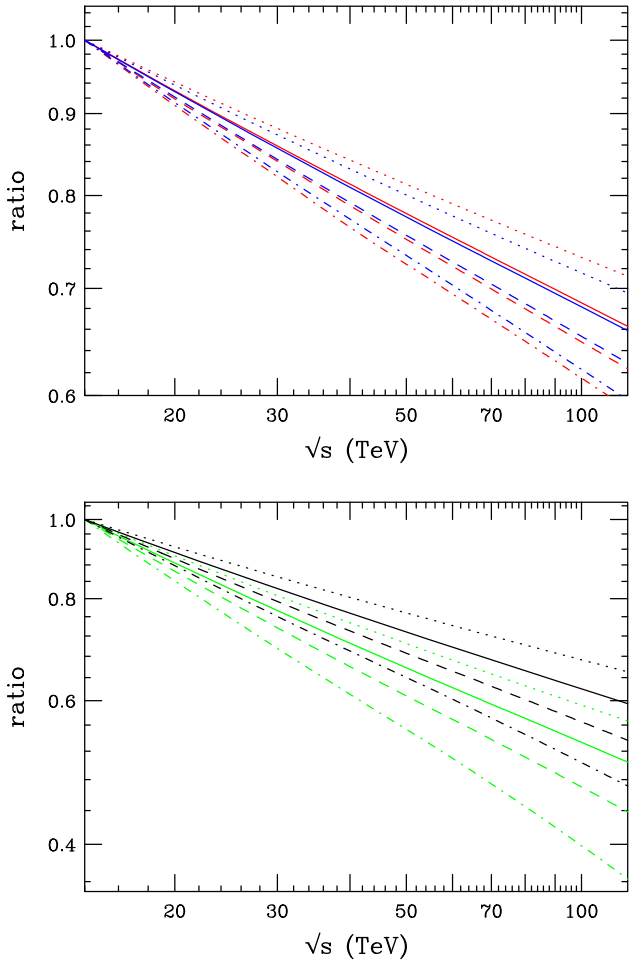

Fig. 1 Ratios of the parton luminosities, defined in the text, as functions of $\sqrt{s}$ in comparison to those at $\sqrt{s} = 14$ TeV. The *dotted* (*solid*, *dashed*, *dash-dotted*) *curves* in all case corresponds to fixed values of $M/\sqrt{s} = 0.3\,(0.4, 0.5, 0.6)$. In the *upper panel* the *red* (*blue*) *curves* corresponds to the $U\bar{U}(D\bar{D})$ cases, respectively, as discussed in the text. In the *lower panel*, the corresponding *green* (*black*) *curves* correspond to the cases gg and gQ, as also discussed in the text, respectively

From the two panels in this figure we learn several important things: (a) the ratio of luminosities in the range of interest scale roughly as $(\sqrt{s})^{-q}$ with $q > 0$ as expected from above, which makes this dependence appear *almost* linear in these log–log plots.[4] The particular value of q depends upon the choice of the colliding partons as well as the specific choice of the value of $M/\sqrt{s}$. (b) In all cases we observe that as $M/\sqrt{s}$ increases so does the value of the 'slope' q. (c) Since the gluon PDF evolves more quickly than do the valence or sea quarks, the slopes in the gg case are seen to be greater than in the corresponding ones in the gQ cases which are themselves greater than the corresponding ones observed in the $U\bar{U}$ and $D\bar{D}$ cases. In particular we see that in the gg

[4] Note q is generally distinct from the parameter p introduced above.

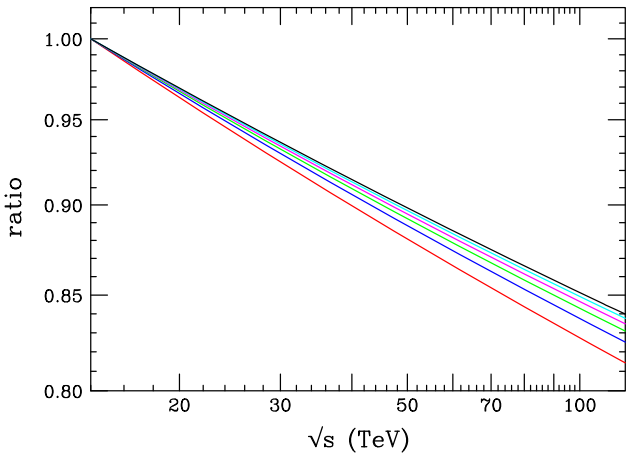

Fig. 2 The ratio of the value of $\alpha_s(M)$, for fixed $M/\sqrt{s}$, as a function of $\sqrt{s}$ to that at 14 TeV. From *bottom* to *top* the *curves* correspond to $M/\sqrt{s} = 0.1$ to 0.6 in steps of 0.1

case the luminosity ratio for $M/\sqrt{s} = 0.6$ falls off by a factor of $\sim$2.5 as $\sqrt{s}$ increases to 100 TeV from 14 TeV due to the Q^2 evolution. This would mean that if *only* the PDFs mattered in the scale breaking then keeping the relative reach of $M/\sqrt{s} = 0.6$ for NP fixed when going from 14 TeV to 100 TeV the luminosity would need to increase by a factor of $\sim$128. (d) The $U\bar{U}$ combination is also seen to evolve somewhat more quickly with $M/\sqrt{s}$ than does the corresponding $D\bar{D}$ PDF combination. Of course, there are *other* sources of scaling violation which can potentially change the value of 'partonic' slope q to that of interest for a specific physical process, p.

In a similar manner one can examine the magnitude of the effect of scaling violations from the running of $\alpha_s(M)$, for fixed values of $M/\sqrt{s}$, by comparing its evolution as $\sqrt{s}$ increases beyond 14 TeV; Fig. 2 shows this result. Here we see that this evolution is (very) roughly constant for reasonable, yet fixed, values of $M/\sqrt{s}$. However, the slope is slightly less steep for larger $M/\sqrt{s}$ values and some non-trivial curvature away from a straight line behavior is clearly visible. How much the running of α_s will contribute to the overall scaling violation in a given process strongly depends upon the power in which it appears in the relevant subprocess cross sections, $\hat{\sigma} \sim \alpha_s^m$. In the cases we will examine below we have $m = 0$, 1 or 2.

3 Sample benchmark new physics scenarios

We now turn to an examination of how the production cross sections and mass reach associated with different specific benchmarks of NP will scale as we increases $\sqrt{s}$ beyond 14 TeV along the lines discussed above by employing the ratio R. This survey is not meant to be in any way exhaus-

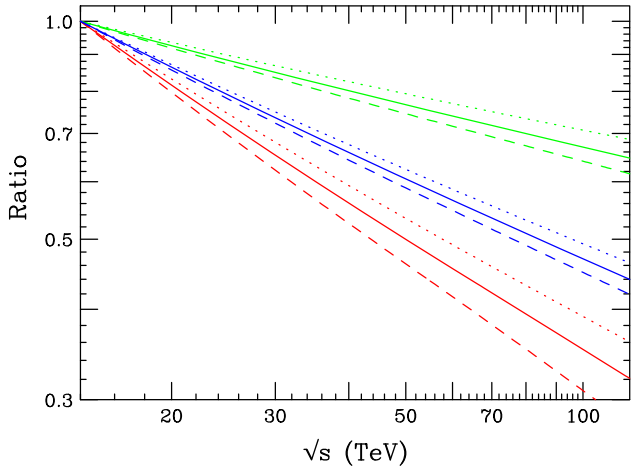

Fig. 3 The ratio R of scaled cross sections defined in the text as functions of $\sqrt{s}$. Here the *dotted* (*solid*, *dashed*) *green curves* corresponds to values of $M/\sqrt{s} = 0.3(0.4,\ 0.5)$ for inclusive $W'^{\pm}$ production followed by leptonic decay with $M = M_{W'}$. The *blue* (*red*) *curves* are for inclusive heavy quark pair production via $q\bar{q}(gg) \to Q\bar{Q}$; in this case M is identified with the heavy quark mass and the *dotted* (*solid*, *dashed*) *curves* correspond to values of $M/\sqrt{s} = 0.15$ (0.20, 0.25), respectively

Table 1 Ratios of the integrated luminosity required at a 100 TeV FHC to maintain the same relative mass reach, $M/\sqrt{s}$, as that at the 14 TeV LHC for various types of NP as discussed in the text

Particle	$M/\sqrt{s}$	L (100)/L (14)
W'	0.30	74.3
W'	0.50	79.6
$Q(q\bar{q})$	0.15	103.6
$Q(q\bar{q})$	0.25	113.5
$Q(gg)$	0.15	130.5
$Q(gg)$	0.25	165.2
L	0.03	59.9
L	0.07	65.9
LQ	0.15	127.9
LQ	0.25	159.4
q^*	0.40	96.5
q^*	0.60	118.8
BH6	0.20	67.8
BH6	0.70	93.0

tive, but only indicative of the possible range of the values of the ratio R and to demonstrate what might be expected from going beyond the naive scaling arguments. Based on the discussion above it is clear that the results we obtain will depend upon which subset of the PDFs are dominant and the role that α_s plays in the relevant NP production process, generally at LO, as NLO and higher order corrections will be sub-leading.

We begin by considering the Drell–Yan production of the $W'^{\pm}$ gauge boson in the sequential SM[5] in the narrow width approximation (NWA) followed by its subsequent leptonic decay. In this case the α_s corrections to both the cross section and leptonic branching fractions appear only at NLO (but are included here) and so the scaling behavior is expected to be dominated by that associated with the U- and D-type PDFs. Figure 3 shows the scaled cross section ratio for this process assuming that $M_{W'}/\sqrt{s} = 0.3$, 0.4 or 0.5. These values were chosen since the expected reach for the SSM W' at the 14 TeV LHC typically lies in the 5–7 TeV range. Indeed, the behavior of the ratio R in this case is observed to generally follow that produced by a weighted combination of that for the $U\bar{U}$ and $D\bar{D}$ PDFs as we see by comparison with the top panel in Fig. 1. This means, e.g., that the required luminosity to maintain the same value of the scaled search reach is only modestly larger than suggested by the scaling estimate. Note that as expected R behaves in all cases roughly as $(\sqrt{s})^{-p}$, *i.e.*, is almost linearly on this log–log plot. Table 1 shows the required integrated luminosity scaling for a $\sqrt{s} = 100$ TeV collider in comparison to the 14 TeV LHC to be in the ∼74–80 range for this process which is *only* ∼50 % larger that than implied by the scaling limit.

Interestingly, if we consider the $\sqrt{s} = 100$ TeV collider as a specific example, it is easy to access the cost in the search reach for the W' if the 'required' integrated luminosity goal is not reached. We find [8] that for integrated luminosities in the 1–1000 ab^{-1} range the discovery reach increases/decreases by ∼7.60 TeV for every factor of 10 of integrated luminosity gained or lost. The search reach is found to be ∼39.1 TeV, assuming 10 ab^{-1} is available, so this is roughly a factor of ∼20 % for an order of magnitude change in luminosity.

A second interesting example is provided by new heavy quark (Q) pair production which proceeds by $gg, q\bar{q}$ fusion at LO. Although the actual cross section for $Q\bar{Q}$ production is a PDF-weighted combination of these two contributions, it is interesting to consider these processes separately since they depend on different PDFs, yet both occur at $O(\alpha_s^2)$ in LO. Figure 3 shows the R ratio for these processes assuming that $M(= M_Q)/\sqrt{s} = 0.15$–0.25 corresponding to $M_Q \sim 2$–3 TeV at the 14 TeV LHC. Here we see that R falls much faster than do the corresponding relevant PDFs in either case due to the additional scaling violation associated with the running of the α_s coupling. Table 1 shows in these cases the required integrated luminosity scaling for a $\sqrt{s} = 100$ TeV collider to be in the ∼103–115 range for the $q\bar{q}$-initiated process and ∼130–165 for the gg-initiated process, which is expected to be dominant at large values of $\sqrt{s}$. If we roughly require 100 signal events at a $\sqrt{s} = 100$ TeV collider as a benchmark signal rate for purposes of comparison (note:

[5] For some overviews of the physics of new gauge bosons and original references, see [4–7].

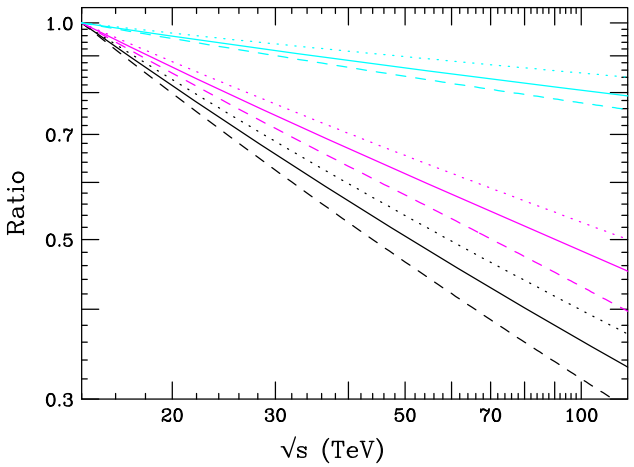

Fig. 4 The ratio R of scaled cross sections defined in the text as functions of $\sqrt{s}$ as in the previous figure. The *cyan curves* are for the production of heavy vector-like, isodoublet lepton pairs, $q\bar{q} \to L^+L^-$ where $M = M_L$ and the *dotted* (*solid*, *dashed*) *curves* correspond to values of $M/\sqrt{s} = 0.03$ (0.05, 0.07), respectively. The *magenta curves* are for the resonant single production of a color-triple excited quark, with $M = M^*$, in gq fusion assuming that $M/\sqrt{s} = 0.4$ (0.5, 0.6) as discussed in the text. The corresponding *black curves* are for scalar, color-triplet leptoquark pair production summed over both the gg and $q\bar{q}$ channels taking $M = M_{LQ}$ and assuming $M/\sqrt{s} = 0.15$ (0.20, 0.25), respectively

not for a discovery or to set a limit) this corresponds to a heavy quark mass of ∼9.42 (12.40, 15,57, 18.82) TeV for integrated luminosities of 1 (10, 100, 1000) ab^{-1}, respectively, which displays how the mass reach scales with luminosity variations in the range of interest. We see that this corresponds to roughly a factor of ∼20 % change in mass reach for an order of magnitude change in the integrated luminosity.

Several more NP processes are considered in Fig. 4 the first being heavy vector-like lepton (L) pair production via $q\bar{q}$ annihilation through γ, Z exchange, ignoring the potential contribution of the gg-fusion, loop-induced process[6] since it is more model dependent. To be specific, we will consider the case of a singly charged, weak isodoublet lepton, as might appear in an E_6-type framework (see, for example, the third paper in Ref. [6]) although the results we obtain are quite independent of this particular choice. Since this production cross section in this case is rather small and searches for such heavy leptons are dominated by large SM backgrounds from inclusive W^+W^- production, we restrict ourselves to rather low leptonic mass values, i.e., $M(= M_L)/\sqrt{s} = 0.03$–0.07, corresponding to heavy lepton masses well below 1 TeV at LHC14. Since these $M/\sqrt{s}$ values are so low and α_s enters only at NLO for this process we expect the $\sqrt{s}$ dependence of R as well as its deviations from unity to be rather weak. This is exactly what we find by looking at Fig. 4. This means, e.g., that the required luminosity to maintain the same value of the scaled search reach is only a bit larger than suggested by the scaling estimate in this scenario. Table 1 shows the required integrated luminosity scaling for a $\sqrt{s} = 100$ TeV collider to be in the ∼60–66 range for such heavy leptons. For a $\sqrt{s} = 100$ TeV collider, and, taking 100 events as a standard for comparison of the potential mass reach, we find this event rate corresponds to heavy lepton masses of ∼400 (625, 904, 1218) GeV assuming luminosities of 1 (10, 100, 1000) ab^{-1} so that variations of a factor of 10 produce a roughly ∼30 % change in the approximate mass reach, a value not too dissimilar from the previous case.

Another example provided by Fig. 4 is that of scalar (spin-0), color-triplet leptoquark (LQ) (for some reviews, see [10–12]) pair production which, like heavy quark production arises from both $q\bar{q}$- and gg-initiated processes which we combine into the total cross section in the presentation below. Since in LO these are also α_s^2 processes but differ in kinematic detail from the corresponding $Q\bar{Q}$ ones (due to their spin-0 nature) we expect results which are similar to but quantitatively different from those found for heavy quark production. This is exactly what we observe in Fig. 4. Table 1 shows in this case the required integrated luminosity scaling for a $\sqrt{s} = 100$ TeV collider to be in the ∼127–160 range for such heavy leptoquarks, a value not very different from that for gg-initiated heavy quark production. For a $\sqrt{s} = 100$ TeV collider, and taking 100 events as a minimal search criterion as above, then the mass reach is found to be ∼6.60 (8.97, 11.70, 14.70) TeV assuming integrated luminosities of 1 (10, 100, 1000) ab^{-1}, so that variations by a factor of 10 in integrated luminosity again produce a roughly ∼30 % change in the mass reach.

A last example shown in Fig. 4 is that of single, resonant, excited quark (q^*) (with mass M_{q^*}) production in $gq(\bar{q})$-fusion[7] which proceeds via an effective dimensional-5 operator with a cross section that is proportional to α_s. Here we also require that the each of the jets from the decay of the q^* satisfy $\eta_j < 0.5$ to reduce the QCD backgrounds. Explicitly, in the NWA one finds that in the case the partonic cross section behaves like $\hat{\sigma} \sim (\alpha_s/\Lambda^2)\ (M_{q^*}^2/s)$ times a product of the appropriate PDFs where Λ is identified with the 'compositeness' scale associated with the dim-5 operator. Provided we keep both $M_{q^*}^2/s$ and Λ^2/s fixed as $\sqrt{s}$ increases, then in the scaling limit the ratio R is again always unity. In the real world, since the cross section only involves a single power of the strong coupling and the relevant PDFs are of the gQ type we expect R to have an intermediate behavior between that observed for heavy quark production and that found for W' production and that is indeed the situation revealed in

[6] gg-Fusion induced heavy lepton production at 1-loop was first considered in [9].

[7] Resonant excited quark production at hadron colliders was first studied in [13].

Fig. 4. Here we assume that $M_{q^*}/\sqrt{s} = 0.4$–0.6, given the present 8 TeV and the anticipated 14 TeV LHC search reaches for excited quarks. Table 1 shows in this case the required integrated luminosity scaling for a $\sqrt{s} = 100$ TeV collider to be in the ∼96–116 range for the heavy excited quark scenario. Interestingly, if we require 100 signal events at a $\sqrt{s} = 100$ TeV collider as a benchmark signal rate as well as $\Lambda = M_{Q^*}$ for simplicity, this corresponds to an excited quark mass of 36.1 (44.7, 52.8, 60.3) TeV for integrated luminosities of 1 (10, 100, 1000) ab^{-1}, which shows how the reach scales with luminosity in the region of interest. This roughly corresponds to a factor of ∼20 % for an order of magnitude change in the integrated luminosity.

A final example of NP that we consider is the production of TeV-scale black holes (BHs) of mass $M_{\rm BH}$ that arise in theories with extra dimension (see, for example, [14,15]). In the simplest toy models with additional flat dimensions, BH production has a simple threshold at the $n + 4$-dimensional Planck mass, M_P, with a continuum above this value, and it has a partonic cross section that scales as $\hat{\sigma}_{\rm BH} \sim (M_{\rm BH}/M_P)^{2/1+n}\ M_P^{-2}$. It is also usually assumed that the products of *all* the PDFs enter here since the collision of any two partons can make a BH with the same efficiency given sufficient collision energy. This implies that the total BH cross section behaves as

$$\sigma_{\rm BH} \sim \int_{\tau_{min}}^{1} {\rm d}\tau \int_{\tau}^{1} {\rm d}x\ \Pi_{ij} \times \left(f_i(x, M^2) f_j(\tau/x, M^2)/x \right) \hat{\sigma}_{\rm BH} \qquad (3)$$

where $\tau_{\rm min} = M_P^2/s$ and so the relevant scaled mass reach to consider in this case is just the quantity $M_P/\sqrt{s}$. The factor Π_{ij} represents the sum over all pair-wise products of the PDFs, f_i, as employed in the previous section. The BH mass is then identified with the resulting partonic invariant mass above the value of M_P. Since the cross section for BH production can in principle be very large but may also experience substantial suppression factors of various kinds, we here consider the wide range of values for $M_P/\sqrt{s} = 0.2$–0.7 and the specific cases of $n = 2, 6$. The results we obtain are only very weakly dependent on the specific value of n, as we see from the curves shown in Fig. 5, but they are dependent on the specific chosen value of $M_P/\sqrt{s}$. Since the pair-wise product of all the PDFs enter here (and there are no α_s factors present), we might roughly expect the behavior of the R ratio in this case to be similar to that of the valence PDFs $U\bar{U}$ and $D\bar{D}$. This is essentially what we see here. Table 1 shows in this case the required integrated luminosity scaling for a $\sqrt{s} = 100$ TeV collider for an $n = 6$ BH to be in the ∼67–93 range. Again, for a $\sqrt{s} = 100$ TeV collider, and taking as usual 100 events as a minimal search criterion, then the mass reach for $n = 6$ is found to be ∼47.3 (54.7, 61.6, 67.9) TeV, assuming luminosities of 1 (10, 100, 1000) ab^{-1}, so that variations of a factor of 10 in integrated luminosity would produce a roughly ∼15–20 % change in the BH mass reach.

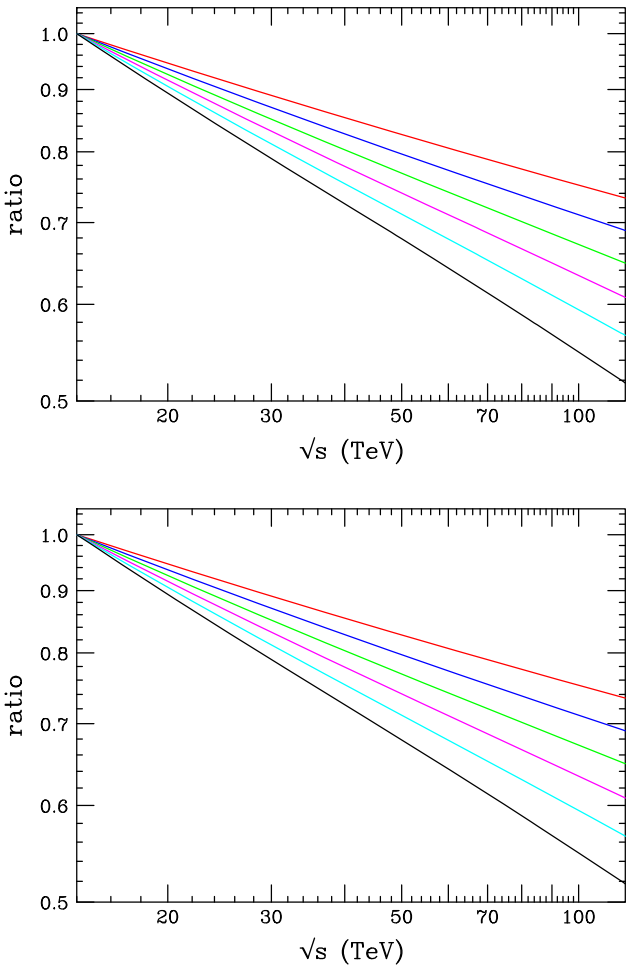

Fig. 5 The ratio R for TeV-scale black hole production assuming $n = 2$ (*top*) or 6 (*bottom*) additional flat dimensions with, from *top* to *bottom*, $M_P/\sqrt{s}$ =0.2–0.7 in steps of 0.1, respectively

4 Luminosity impact on reaches

In this section we will briefly examine the impact of achieving luminosities different from those required to maintain the mass reach scaling law discussed above; to be specific we consider the case of a $\sqrt{s} = 100$ TeV collider. This issue is most easily analyzed by considering the mass reach results shown in Figs. 6 and 7 which employ the same physics examples discussed above. Specifically, these figures show how the mass reaches for the six new physics scenarios considered in the previous section will scale with the integrated luminosity achieved. As alluded to above, we see that in all cases the mass reach is found to depend almost linearly, roughly speaking, on the log of the luminosity in the range of inter-

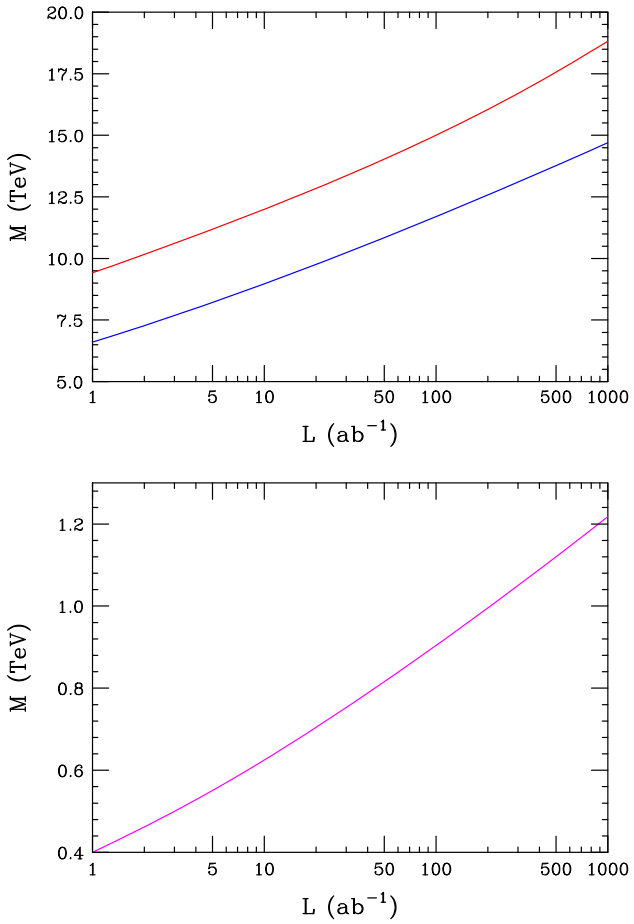

Fig. 6 Luminosity dependence of the various mass reaches discussed in the previous section for a $\sqrt{s} = 100$ TeV collider. The *top panel* shows this dependence for scalar leptoquarks (*blue*) and heavy quarks (*red*), while the *lower panel* shows that for vector-like leptons produced in $q\bar{q}$ collisions.

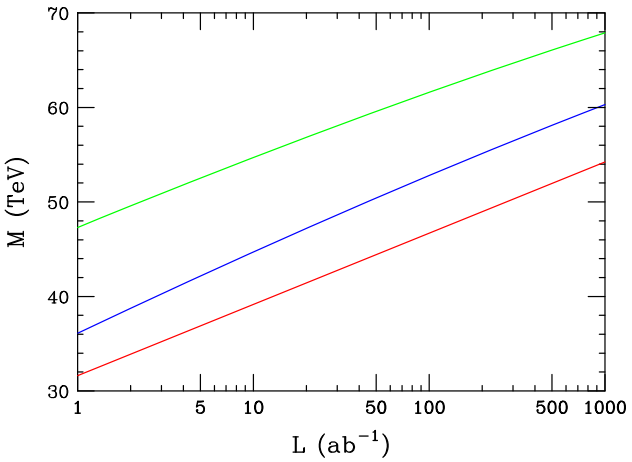

Fig. 7 Same as the previous figure, but now, from *top* to *bottom*, for a $n = 6$ BH, an excited quark and for a SSM W'

Table 2 Comparison of the mass reaches in TeV for various NP scenarios at a $\sqrt{s} = 100$ TeV collider assuming an integrated luminosity of 1 and 100 ab^{-1}, very roughly the average value required for mass reach scaling

Particle	1 ab^{-1}	100 ab^{-1}
W'	31.6	46.7
Q	9.42	15.57
L	0.40	0.90
LQ	6.60	11.70
q^*	36.1	46.7
BH6	47.3	67.9

est. The important point demonstrated by these two figures is that even if there is *no* luminosity gain whatsoever over the LHC, the mass reach of a $\sqrt{s} = 100$ TeV collider is still quite good.

To make an even more direct comparison, we note in Table 1 the mass reaches for these six NP scenarios for a $\sqrt{s} = 100$ TeV collider assuming integrated luminosities of 1 ab^{-1}, comparable to the 14 TeV LHC and so no gain in luminosity, and for 100 ab^{-1}, which is very roughly the average value of the luminosity required to maintain mass reach scaling as are given in Table 2. In a sense, this might be considered to be the worst-case scenario. Here, we see explicitly that the mass reach reduction experienced in this rather extreme situation, due to a factor of 100 times less integrated luminosity, is in all but one scenario (where the factor of 100 employed is too large) is less than 30–40 %. Thus we conclude that, while not reaching the desired value of the integrated luminosity given by the scaling requirement does result in a reduction in mass reach, it is found to be not a very serious loss for the NP scenarios considered here. Of course, more detailed work needs to be done to more fully understand the impact of a reduced integrated luminosity on the various NP searches.

5 Discussion and conclusions

Proposed future hadron colliders will have a vastly improved mass reach for new physics in comparison to that of the 14 TeV LHC. In this paper we have examined how the required integrated luminosity for such machines must scale in order to maintain the same *relative* mass reach, $M/\sqrt{s}$, as at the LHC for various kinds of new physics benchmark models as $\sqrt{s}$ increases beyond 14 TeV. For a $\sqrt{s} = 100$ TeV collider, the scaling limit requires the integrated luminosity to be ∼50 times larger than at the 14 TeV LHC for *all* types of NP and for *all* fixed values of $M/\sqrt{s}$. In contrast to this, due to inherent scaling violations of the PDFs and, in some cases that of the strong coupling, α_s, we obtain a rather wide range of possible values, ∼60–165, for various kinds of NP benchmarks and for different assumed values of $M/\sqrt{s}$.

All of these integrated luminosity values are larger, and in some cases significantly larger, than that given by the scaling argument. The costs of reaching these types of integrated luminosity goals will be quite high and it will be up to further detailed studies to decide how well they can or should be met at any future hadron collider. Here we have made some crude estimates that indicate that in all the NP scenarios examined a reduction in the integrated luminosity by one (two) order(s) of magnitude around the relevant NP mass ranges of interest would result in a search reach degradation of, roughly, only $\sim$15–30 (30–40) % for a $\sqrt{s} = 100$ TeV collider. However, even if only this lower luminosity were to be achieved, the gain in mass reach obtained by going to larger values of $\sqrt{s}$ remains very substantial.

Acknowledgments The author would like to thank both M. Breidenbach and particularly B. Richter for continually emphasizing to him the importance of the luminosity scaling issue for future hadron colliders and pushing this project along. He would also like to thank J. L. Hewett for many discussions related to the NP choices made in this analysis as well as Ken Lane for more general discussions. This work was supported by the Department of Energy, Contract DE-AC02-76SF00515.

References

1. B. Richter, Rev. Accel. Sci. Tech. **7**, 1 (2014). arXiv:1409.1196 [hep-ex]
2. E. Eichten, I. Hinchliffe, K.D. Lane, C. Quigg, Rev. Mod. Phys. **56**, 579 (1984) [Addendum-ibid **58**, 1065 (1986)]
3. L.A. Harland-Lang, A.D. Martin, P. Motylinski, R.S. Thorne, arXiv:1412.3989 [hep-ph]
4. P. Langacker, Rev. Mod. Phys. **81**, 1199 (2009). arXiv:0801.1345 [hep-ph]
5. M. Cvetic, S. Godfrey, in Electroweak Symmetry Breaking and New Physics at the TeV Scale. arXiv:1307.7292, ed. by Barklow, T.L., et al., pp. 383–415. arXiv:hep-ph/9504216
6. J.L. Hewett, T.G. Rizzo, Phys. Rep. **183**, 193 (1989)
7. T.G. Rizzo, arXiv:hep-ph/0610104
8. T.G. Rizzo, Phys. Rev. D **89**(9), 095022 (2014). arXiv:1403.5465 [hep-ph]
9. S.S.D. Willenbrock, D.A. Dicus, Phys. Lett. B **156**, 429 (1985)
10. W. Buchmuller, R. Ruckl, D. Wyler, Phys. Lett. B **191**, 442 (1987) [Erratum-ibid. B **448**, 320 (1999)]
11. M. Leurer, Phys. Rev. D **49**, 333 (1994). arXiv:hep-ph/9309266
12. J.L. Hewett, T.G. Rizzo, Phys. Rev. D **56**, 5709 (1997). arXiv:hep-ph/9703337
13. U. Baur, I. Hinchliffe, D. Zeppenfeld, Int. J. Mod. Phys. A **2**, 1285 (1987)
14. S.B. Giddings, S.D. Thomas, Phys. Rev. D **65**, 056010 (2002). arXiv:hep-ph/0106219
15. S. Dimopoulos, G.L. Landsberg, Phys. Rev. Lett. **87**, 161602 (2001). arXiv:hep-ph/0106295 [Here we employ the numerical conventions as given in T.G. Rizzo, JHEP **0506**, 079 (2005). arXiv:hep-ph/0503163]